

UC Irvine

UC Irvine Previously Published Works

Title

Experimental study of cryogen spray properties for application in dermatologic laser surgery

Permalink

<https://escholarship.org/uc/item/60k6n2z9>

Journal

IEEE Transactions on Biomedical Engineering, 50(7)

ISSN

0018-9294

Authors

Aguilar, G
Majaron, B
Karapetian, E
[et al.](#)

Publication Date

2003-07-01

DOI

10.1109/tbme.2003.813537

Copyright Information

This work is made available under the terms of a Creative Commons Attribution License, available at <https://creativecommons.org/licenses/by/4.0/>

Peer reviewed

Experimental Study of Cryogen Spray Properties for Application in Dermatologic Laser Surgery

Guillermo Aguilar*, Boris Majaron, Emil Karapetian, Enrique J. Lavernia, and J. Stuart Nelson

Abstract—Cryogenic sprays are used for cooling human skin during laser dermatologic surgery. In this paper, six straight-tube nozzles are characterized by photographs of cryogenic spray shapes, as well as measurements of average droplet diameter, velocity, and temperature. A single-droplet evaporation model to predict average spray droplet diameter and temperature is tested using the experimental data presented here. The results show two distinct spray patterns—sprays for 1.4-mm-diameter nozzles (*wide nozzles*) show significantly larger average droplet diameters and higher temperatures as a function of distance from the nozzle compared with those for 0.5–0.8-mm-diameter nozzles (*narrow nozzles*). These results complement and support previously reported studies, indicating that *wide nozzles* induce more efficient heat extraction than the *narrow nozzles*.

Index Terms—Droplet size, nozzle geometry, skin cooling.

I. INTRODUCTION

LASER treatment of hypervascular skin lesions, such as port wine stain birthmarks, is the clinical application of interest in this work, and several papers summarize the progress to date [1]–[3]. To remove these lesions, patients are treated with laser pulses that induce permanent thermal damage to targeted blood vessels, typically located 200–550 μm below the skin surface. However, nonspecific absorption of laser energy by epidermal melanin, localized within the most superficial skin layer, can lead to undesirable damage such as scarring or dyspigmentation [4]. To prevent thermal injury to the epidermis, short spurts of cryogen are sprayed on the skin prior to laser exposure [5]. In order to achieve optimal cooling of the epidermis with minimal cooling of the subsurface target, it is necessary to control precisely the cryogen spurt

Manuscript received April 1, 2002; revised December 27, 2002. This work was supported by the Whitaker Foundation, by Candela Corporation under Grant 482560-59109, by the National Institutes of Health under Grants GM-62177, AR-47551, and HD-42057, by the National Science Foundation under Grant CTS-9901375, by the Office of Naval Research, by the National Institutes of Health, and by the Beckman Laser Institute Endowment. The work of B. Majaron was supported by the Slovenian Ministry of Education and Science. *Asterisk indicates corresponding author.*

*G. Aguilar is with the Department of Biomedical Engineering, University of California, Irvine, CA 92697 USA, and also with the Beckman Laser Institute, University of California, Irvine, CA 92612 USA (e-mail: gaguilar@bli.uci.edu).

B. Majaron is with the Beckman Laser Institute, University of California, Irvine, CA 92612 USA, and also with the Jožef Stefan Institute, SI-1000 Ljubljana, Slovenia.

E. Karapetian is with the Beckman Laser Institute, University of California, Irvine, CA 92612 USA, and also with the Department of Chemical Engineering and Material Sciences, University of California, Irvine, CA 92697 USA.

E. J. Lavernia is with the Department of Chemical Engineering and Material Sciences, Irvine, CA 92697 USA.

J. S. Nelson is with the Department of Biomedical Engineering, University of California, Irvine, CA 92697 USA, and also with the Beckman Laser Institute, University of California, Irvine, CA 92612 USA.

Digital Object Identifier 10.1109/TBME.2003.813537

duration [6] and spray properties. Although technology for cryogen-spray-cooling (CSC)-assisted laser therapy has been commercially available for several years, only a few studies have focused on measuring systematically the properties of cryogen sprays produced by different nozzle geometries [7]–[10]. Further studies are needed to better understand how spray properties could be modified to obtain optimum cooling efficiency and selectivity.

In this paper, the dependence of spray properties on nozzle geometries and their variation as a function of distance from the nozzle are studied by characterizing cryogen sprays from six different nozzles. First, the effect of nozzle diameter (D_N) and length (L_N) on spray shape is observed using fast-flashlamp photography. Then, the average droplet diameter D , velocity V , and temperature T are measured at various distances from the nozzle tip z . Subsequently, we compare our experimental results of D and T with an earlier developed single-droplet evaporation model [11]. Finally, our experimental results are discussed in the context of those obtained during recent studies aimed at measuring the heat extraction from skin during CSC [12]–[14].

II. EXPERIMENTAL SYSTEMS AND PROCEDURES

A. Spray Forming Systems

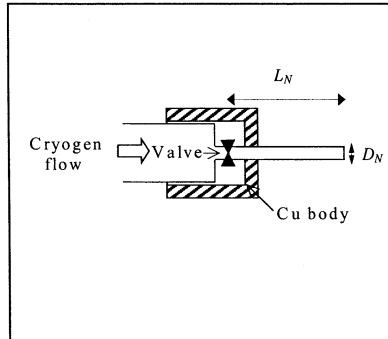
The cryogen utilized in the present study is 1,1,1,2 tetrafluoroethane (R-134a) with a boiling temperature T_b of -26°C at atmospheric pressure. This is the only FDA approved cryogen for laser dermatologic surgery. The cryogen is kept in a container at a saturation pressure of 660 kPa (95.7 psi) at 25°C , and delivered through a standard high-pressure hose to the nozzles under study via a fuel injector, used to control electronically the spurt duration.

In some previous studies [2], [8], fuel injectors without nozzle attachments have been used. However, we have observed and it has also been reported [8] that fuel injectors without nozzles may produce hollow cone sprays, which would undoubtedly induce inhomogeneous heat extraction that would be undesirable for applications of CSC in dermatologic laser surgery. For this reason, the present study was carried out using only fuel injectors with nozzle attachments. Four straight-tube nozzles with two different lengths (L_N) and two different inner diameters (D_N), and two commercial nozzles used for clinical laser treatment (ScleroPLUS and GentleLASE, Candela Corporation, Wayland, MA) were studied. Table I shows the dimensions of all six nozzles under study and the terms used to identify them.

B. Spray Shape and Droplet Diameter

A progressive-scan CCD camera with a shutter speed of 60 μs was used to photograph the spray shapes. A flash lamp provided illumination gating by 5- μs pulses that “freeze in” the image

TABLE I
DESIGN SPECIFICATIONS FOR NOZZLES UNDER STUDY



Nozzle	L_N [mm]	D_N [mm]	L_N/D_N
Short wide (SW)	31.8	1.4	23
Long wide (LW)	63.5	1.4	46
Short narrow (SN)	31.8	0.7	46
Long narrow (LN)	63.5	0.7	93
ScleroPLUS™ (SP)	25.4	0.8	33
GentleLASE™ (GL)	18.0	0.5	35

of moving cryogen droplets. Twelve spray shape images were captured for each nozzle at an acquisition rate of 30 frames per second.

An Ensemble Particle Concentration & Sizing apparatus (EPCS, Insittec/Malvern, Worcestershire, U.K.) was used to measure average droplet diameter (D). The operating principle of this apparatus is based on low angle laser light scattering (LALLS). The light scattered by spray droplets is collected by a set of 30 concentric ring detectors capable of measuring over a droplet diameter range of 2–200 μm with 3% accuracy, according to the manufacturer. To determine droplet diameter from the input signals, EPCS uses a computer program (RT Sizer, Insittec/Malvern, Worcestershire, U.K.), which is based on the Mie theory of light-particle interactions. A more detailed description of this apparatus may be found elsewhere [15]. The laser beam diameter of this apparatus is normally 10 mm, but using an inverted beam expander, it was reduced to 3.3 mm to obtain a smaller probe cross section. Measurements were taken along the centerline of the spray cone at various distances from the nozzle with a minimum separation of 5 mm. A realistic estimate of the experimental error of our measurements is 15%–20%.

We use Sauter mean diameter (SMD or D_{32}) as a meaningful quantity of droplet diameter. SMD represents an average droplet diameter with the same volume to surface area ratio as that of the entire spray. For fuel combustion applications, Lefebvre [16] highly recommends the use of this average diameter, since it is least susceptible to a large spread in the droplet diameter distribution. Since cryogen and fuel sprays are made of droplets evaporating in flight, it seems appropriate to use SMD in the present work.

C. Droplet Velocity and Spray Development Time

To estimate an average droplet velocity, we used a simple experimental time-of-flight procedure (TFP), utilizing a continuous laser beam (He–Ne laser, 633 nm) aimed at a fast

photodetector [Fig. 1(a)]. A digital oscilloscope records the output signal of the photodetector, which decreases when spray droplets obstruct the beam. Fig. 1(b) shows an example where the LN nozzle tip was positioned at $z_2 = 60$ mm from the laser beam and a Δt_2 of 5 ms was measured.

By repeating such measurements at two known distances from the spray nozzle (z_1 and z_2), an overall droplet velocity ($V_{1,2}$) can be computed from the difference in delays between input from the digital delay generator and first signs of attenuation of the photodetector signal (Δt_2 and Δt_1), i.e., $V_{1,2} = (z_2 - z_1)/(\Delta t_2 - \Delta t_1)$. It is important to note that $V_{1,2}$ represents the velocity of the fastest moving droplets, averaged over the distance interval (z_1 to z_2). Considering all sources of error for this technique, we estimate a ± 5 m/s uncertainty in our $V_{1,2}$ measurements.

In addition to estimating $V_{1,2}$, this procedure allows determination of the spray development time (t_d). This is the time required for the spray to reach steady-state conditions and can be estimated from the time difference between the point where the photodetector signal starts to diminish, and that where the signal stalls around a lower mean value. In the example shown here [Fig. 1(b)], a t_d value on the order of 20 ms was measured.

D. Temperature Measurements

A type-K thermocouple with a 0.3-mm bead diameter was used to measure average spray temperature T . The thermocouple was supported by a rigid stick and inserted into the center of the spray cone at varying distances z from the nozzle. Since water condensation and freezing can affect temperature measurements, these experiments were conducted in a chamber filled with dry air (relative humidity below 5%) [17].

III. RESULTS

Fig. 2 shows photographs of fully developed (i.e., steady-state) sprays produced by the six nozzles under study. For the SW and LW nozzles, cryogen exits the nozzle in

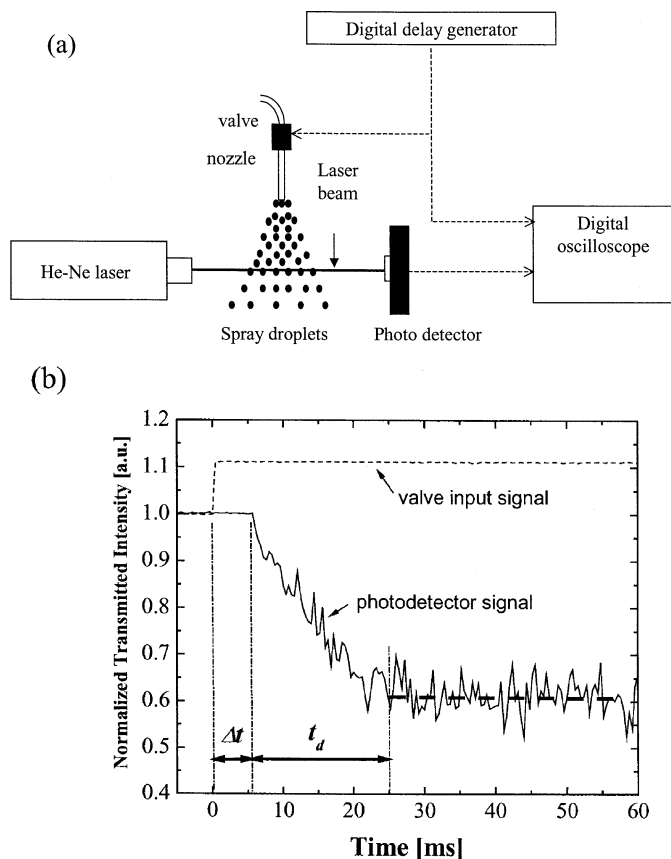


Fig. 1. (a) Sketch of time of flight procedure (TFP) setup. (b) Normalized valve input and photodetector signals. In this example, the LN nozzle tip was positioned at $z_2 = 60$ mm from the laser beam during a 100-ms cryogen spurt. The solid line represents the photodetector signal, and the dashed line represents the valve input signal. The time interval between the first signs of intensity attenuation of the photodetector signal and that when the signal stalls around an average lower value is referred to as spray development time (t_d), which is 20 ms for this example.

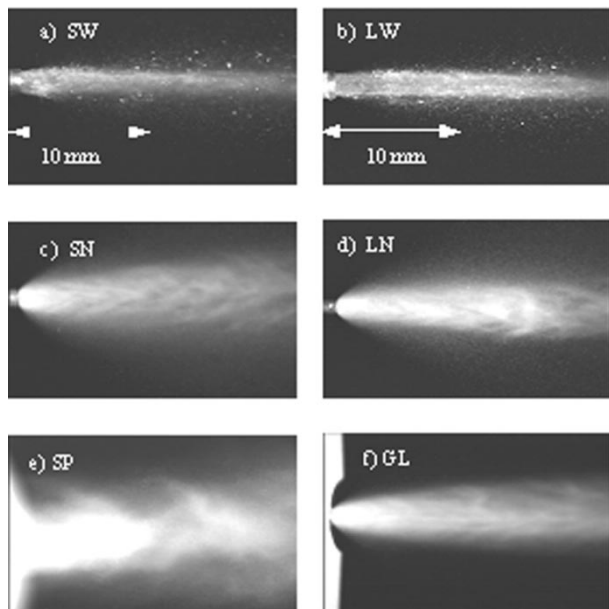


Fig. 2. Photographs of cryogenic spray shapes produced by the nozzles. Length of field of view is 17 mm.

a jet-like fashion [Fig. 2(a) and (b)], compared with the SN and LN nozzles, for which a more pronounced cone angle and more

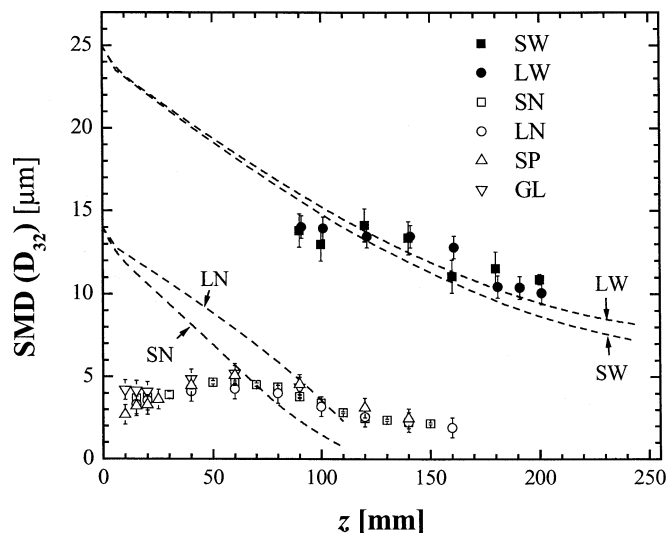


Fig. 3. SMD measurements using the EPCS Insitec/Malvern apparatus. Dashed lines represent SMD predicted by the model for all nozzles. The initial values used in the model for V_0 are 80, 60, 30, and 15 m/s for SW, LW, SN, and LN, respectively; and for D_0 are 25 and 14 μm for wide and narrow nozzles, respectively.

finely atomized spray is noted [Fig. 2(c) and (d)]. Although the influence of L_N on spray shape is less apparent than the effect of D_N , the somewhat higher intensity of the reflected light seems to indicate a denser spray core with longer nozzles. Photographs of the SP and GL sprays show large differences in their patterns [Fig. 2(e) and (f)]. However, the SP handpiece housing partially obstructs the spray causing some droplet scatter [Fig. 2(e)]. When the housing is removed, the spray shape is similar to that of SN, LN, and GL nozzles. Based on these photographs, it appears reasonable to distinguish between “jet-like” and coarsely atomized sprays, produced by wide nozzles with $D_N = 1.4$, and the cone-like, finely atomized sprays produced by narrow nozzles with $D_N = 0.5\text{--}0.8$ mm.

Fig. 3 shows SMD measurements using the EPCS instrument. Solid and hollow symbols illustrate results for the wide and narrow nozzles, respectively. Error bars representing standard deviations of a total of three to five measurements at the same z are included on each data point. The first characteristic noted is that there is practically no variation in D between the wide nozzles, and between the narrow nozzles, within the range of z measured. A two-sample independent t -test between the measurements of the wide and narrow nozzle sprays yields a P-value < 0.01 , demonstrating that the difference in D of these two spray groups is statistically significant at a 95% level. These measurements confirm the existence of two atomization patterns, as suggested above: larger droplet diameters (10–15 μm) produced by the wide nozzles, and smaller droplet diameters (2–6 μm), produced by the narrow nozzles. Also shown in Fig. 3 (dashed lines) are the droplet diameters predicted using a single-droplet evaporation model [11]. As may be seen, the model predictions of D describe the experimental data reasonably well for the wide nozzles at $z > 100$ mm. The rather large discrepancy at shorter z and, in particular, with the narrow nozzles is discussed in the following section.

Fig. 4 shows results of the TFP experiments performed with the four straight-tube nozzles, at $z = 3, 33, 63, 123,$ and 153 mm. At each location, eight spurts were averaged to

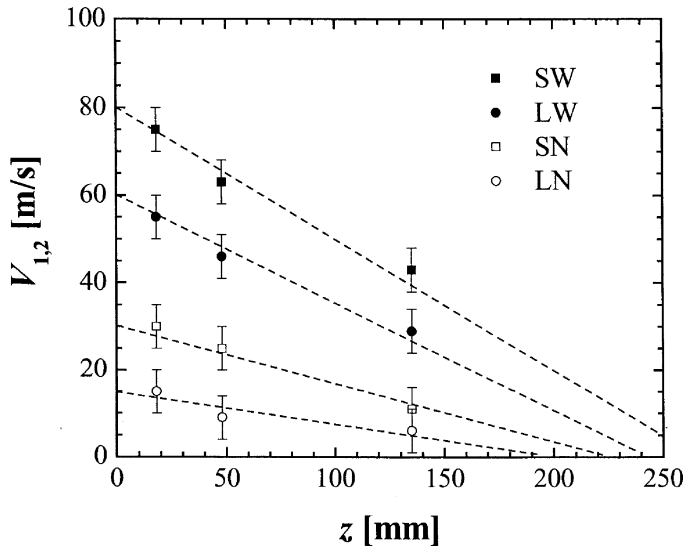


Fig. 4. Average droplet velocity evolution with distance from the nozzle tip for the *wide* and *narrow* nozzles determined by TFP. Dashed lines represent linear regressions where the intercept is forced to rounded values of 80, 60, 30, and 15 m/s for the SW, LW, SN, and LN nozzles, respectively, and is used to determine the initial velocity (V_0) for all nozzles.

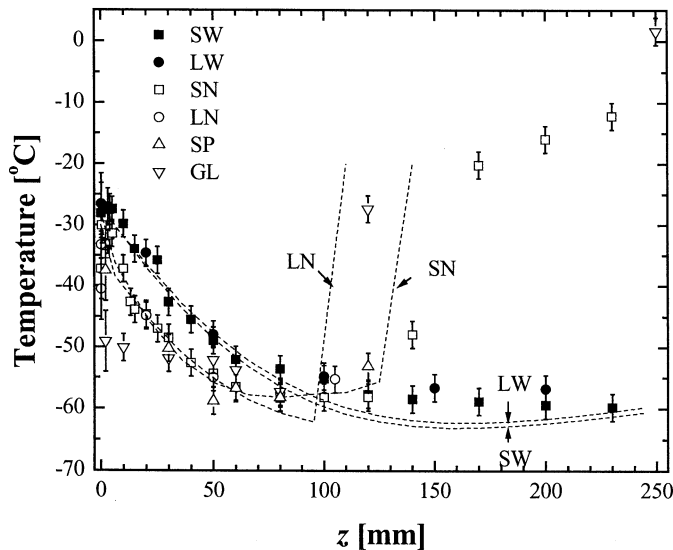


Fig. 5. Measurements (symbols) and model predictions (dashed lines) of spray temperatures (T) as a function of distance from the nozzle (z). The initial values used in the model are $V_{0,SW} = 80$ m/s, $V_{0,LW} = 60$ m/s, $V_{0,SN} = 30$ m/s and $V_{0,LN} = 15$ m/s; $D_{0,-W} = 25$ μ m and $D_{0,-N} = 14$ μ m; and $T_{0,-W} = -26$ $^{\circ}$ C and $T_{0,-N} = -29$ $^{\circ}$ C.

smooth out large oscillations due to turbulence in individual signals. The computed velocities are plotted in Fig. 4 against the mid distances between the 3 to 33, 33 to 63, and 123 to 153 mm ranges, i.e., 18, 48, and 138 mm. The error bars originate from uncertainty in determination of the time delay Δt [see Fig. 1(b)].

Fig. 5 shows average spray temperature T as a function of z measured using a bare thermocouple. Solid and hollow symbols represent the values obtained for the *wide* and *narrow* nozzles, respectively. Error bars represent standard deviations from a total of three to five measurements at the same z . Similarly, as in the photographs and droplet diameter measurements described above, there is practically no variation in T between

the *wide* nozzles, and between the *narrow* nozzles, within the range of z measured. A two-sample independent t test between the measurements of the *wide* and *narrow* nozzle sprays yields a P-value of ~ 0.01 , demonstrating that the difference in T between these two spray groups is also statistically significant at a 95% level. Also shown in Fig. 5 (dashed lines) are the spray temperatures predicted by the single-droplet evaporation model [11], which will be discussed below.

IV. DISCUSSION

Based on photographs of spray shapes (Fig. 2), it is apparent that nozzle length (L_N) does not have a significant impact on overall spray shape, and that nozzle diameter (D_N) ultimately dictates the spray properties, despite the partial spray atomization that the valve itself may induce. These qualitative observations are confirmed by average droplet diameter (Fig. 3) and temperature (Fig. 5) measurements, which show strong similarities between the sprays produced by *wide* nozzles with $D_N = 1.4$ mm and, similarly, between those produced by *narrow* nozzles with $D_N = 0.5$ – 0.8 mm.

Using EPCS, it was not possible to obtain reliable diameter measurements closer than 90 mm from the tip for the *wide* nozzles (Fig. 3), most likely because the spray density was too high [Fig. 2 (a) and (b)]. In contrast, for *narrow* nozzles, it was possible to obtain diameter measurements as close as $z = 15$ mm, because such sprays were better atomized [see Fig. 2(c) and (d)]. The $D(z)$ of *narrow* nozzle sprays clearly show a maximum at 60–70 mm, and a twofold increase in D within the first 50 mm from the nozzle tip. This behavior suggests the presence of droplet coalescence, as observed earlier in liquid and metal sprays [18], [19]. Similarly, the experiments with *wide* nozzles indicate a slight increase in D , or at least a tendency for that value to remain constant in the range of z from 90 to 150 mm. Interestingly, the ratio between the nozzle diameters of the SN (or LN), and GL is 1.4, yet there is no significant difference in their spray shapes, droplet diameter, and temperature. Alternatively, the slightly larger ratio between the *narrow* and *wide* nozzle diameters (2.0) introduces substantial differences in spray shapes, droplet diameter, and temperature, indicating that there is a critical nozzle diameter between 0.8 and 1.4 mm where a large change in the atomization pattern occurs.

The dashed curves shown in Fig. 3 are predictions of the single-droplet evaporation model [11], which requires the input of the initial average droplet diameter (D_0), initial velocity (V_0), and initial temperature (T_0). These parameters must be selected to match the experimental data or deduced from theoretical assumptions. For these experiments, a value of $D_0 = 25$ μ m for the *wide* nozzles produced the best fit within $z = 90$ – 200 mm. In contrast, there was a large mismatch for the *narrow* nozzle sprays, regardless of the value of D_0 chosen (Fig. 3). This is a clear indication that the single-droplet evaporation model is not sufficiently accurate to describe droplet diameter for all sprays under the conditions used for our studies.

Using fast photography, Pikkula *et al.* [8] reported SMD measurements for various nozzles. Exact comparisons of average droplet sizes are difficult since nozzles are not the same, except for the SP nozzle. For this nozzle, their reported SMD value

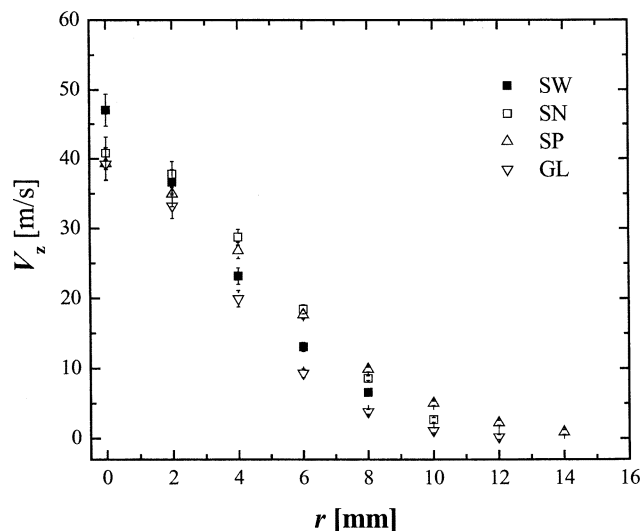


Fig. 6. PDPA local velocity measurements taken at various locations across the spray cone radius at a fixed $z = 60$ mm. Each measurement represents a local average of the axial velocity component (V_z).

is $38.3 \mu\text{m}$ at $z = 40$ mm, while our SMD measurement is $4.46 \pm 0.6 \mu\text{m}$ (~ 9 times smaller). We believe that the difference could be due to the fact that the photographic images used by Pikkula *et al.* were only resolving droplet diameters larger than $9.5 \mu\text{m}$. According to our data, this size limit leaves out the lower half of the total range of droplet diameters measured by our EPCS system. Also, since their measurements focused on the centerline of the spray, the large fraction of smaller droplets that exist near the periphery could not be captured, leading to an overestimated droplet diameter.

Although not shown here, droplet size distributions measured by EPCS showed a small fraction of large droplet diameters ($> 25 \mu\text{m}$) for the *wide* nozzle sprays, while they were almost nonexistent for *narrow* nozzle ones. This is in accordance with the spray photographs, which show a few large droplets near the *narrow* nozzle sprays' periphery [Fig. 2 (a) and (b)] and, also, with the larger SMD values measured for the *wide* nozzles as compared to those of the *narrow* nozzles.

It should also be noted that there is a small effect of L_N on droplet diameter for both the *wide* and *narrow* nozzles (Fig. 3), where D is smaller for shorter nozzles. This is also supported by the TFP velocity measurements (Fig. 4), where $V_{1,2}$ is always greater for shorter nozzles. Although the cryogen vessel pressure is constant, V_0 can differ between nozzles of the same D_N since the shorter nozzles induce less drag on the cryogen flows, yielding a higher V_0 (Fig. 4). Higher velocity droplets enhance the evaporation rate due to increased convection, thus yielding smaller droplet diameters.

Overall spray measurements such as D and $V_{1,2}$ provide insight into the mechanisms of cryogen spray atomization and evaporation. However, in order to understand in more detail phenomena such as droplet coalescence, it is necessary to observe the temporal and local variations in the spray properties. For this purpose, we have conducted preliminary measurements of local droplet velocity using a phase Doppler particle analyzer (PDPA, TSI Inc., St. Paul, MN). This apparatus is based on the principles of light scattering interferometry, and permits simultaneous droplet diameter and velocity measurements over a small

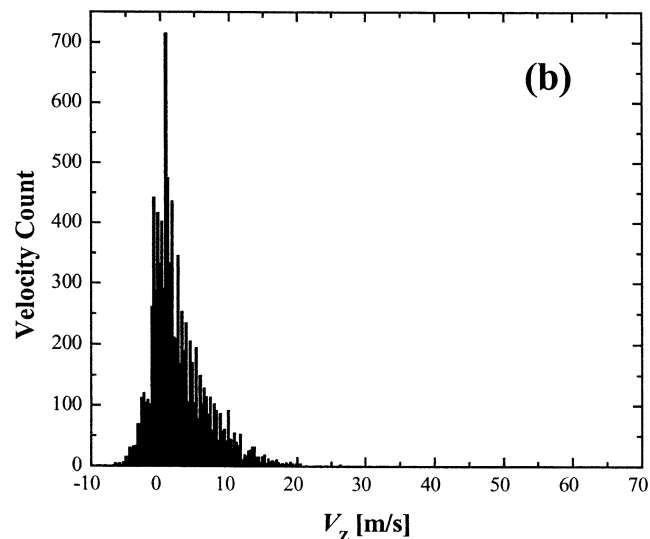
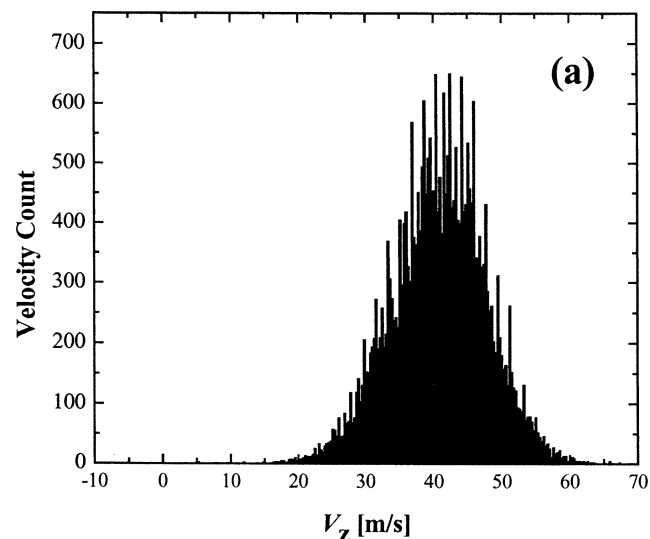


Fig. 7. (a) Velocity distribution of the axial velocity component at the cone's centerline ($r = 0$) at $z = 60$ mm for the SN nozzle. (b) Velocity distribution of the axial velocity component at the cone's edge ($r = 8$ mm) at the same distance z and same nozzle.

($\sim 1 \text{ mm}^3$) probe volume formed by the intersection of two off-phase laser beams of the same wavelength. A more detailed description of this apparatus can be found elsewhere [20].

In Fig. 6, PDPA velocity measurements taken at various locations across the spray cone at $z = 60$ mm are shown for four nozzles (SW, SN, SP, and GL). Each measurement represents a local average of the axial velocity component (V_z) of $\sim 10^3$ – 10^4 droplets in a fully developed spray. The large velocity gradient across the spray cone is accompanied by a noticeable shift in the velocity distribution, as shown by the measurements carried out at the spray cone centerline $r = 0$ [Fig. 7(a)] and near the periphery $r = 8$ mm [Fig. 7(b)], both at $z = 60$ mm and for the SN nozzle. The velocity distribution at $r = 0$ is practically symmetric, centered at ~ 42 m/s with a spread of ± 20 m/s, while that at $r = 8$ mm is markedly skewed, with a maximum at ~ 2 m/s and a spread of -7 and $+18$ m/s. Most distinctly, a relatively large fraction of droplets show negative V_z near the cone's edge, which demonstrates the presence of recirculation zones. Although not conclusive, note that these measurements

were taken at $z = 60$ mm, which is the same distance at which D is maximal for this nozzle (Fig. 3). It is likely that the recirculation zones aids to collisions and coalescence of droplets, as described earlier. We are presently conducting systematic studies to address these issues.

The variation of $T(z)$ for all nozzles shown in Fig. 5 is very consistent with the model predictions (dashed lines). The much poorer match for $D(z)$ suggests that the temperature variation is rather insensitive to variations in $D(z)$. For more finely atomized sprays, which have a larger surface area, removal of latent heat of vaporization from the droplets is more effective, and thus lower temperatures are achieved. In the single-droplet evaporation model, T_0 is adjusted until $T(z)$ best fits the experimental data in the range of $10 < z < 100$ mm. At $z > 100$ mm, the temperature data are somewhat higher than those predicted by the model, likely indicating release of latent heat from water vapor deposited on the thermocouple bead [21]. Indeed, signs of condensation and frost formation on the bead were noted at $z > 100$ mm, despite performing the measurements in a dry atmosphere with relative humidity below 5%. For *wide* and *narrow* nozzles, the best fits are found at $T_0 = -26$ °C and -29 °C, respectively, yielding best predictions for distances up to 90 or 120 mm, where a sudden rise in temperature indicates complete droplet evaporation, in perfect agreement with experimental results (Fig. 5).

Note that the initial temperature estimate (T_0) for *wide* nozzles coincides with the cryogen boiling temperature ($T_b = -26.2$ °C), which is the expected temperature after sudden expansion through the valve, provided that evaporation within the hose and nozzle are negligible. Alternatively, the somewhat lower T_0 estimated for *narrow* nozzles (-29 °C) may indicate some evaporation within the nozzle and consequently better atomization at the nozzle exit. Such an interpretation is consistent with the spray photographs (Fig. 2), which show finer atomization with the *narrow* nozzles.

The present results relate to recent studies, which demonstrated a significant difference between the interface heat transfer coefficient (h) values obtained with the two distinctive spray patterns discussed in this work, namely, values around 10 800 and 7200 W/m² · K for the SW and SN nozzles, respectively [14]. Verkruysse *et al.* [12] attributed similar differences to a buildup of a liquid cryogen layer on the sprayed surface, which—being thicker for *narrow* nozzle sprays—impairs heat extraction efficiency more than with the *wide* nozzle sprays. Based on fast-flashlamp photography of sprays and preliminary surface heat flux (q) measurements, the authors hypothesized [12] and later confirmed [13], that the greater impact of larger and faster droplets, such as those produced by *wide* nozzles, may partly or completely remove the liquid cryogen layer and, consequently, extract heat from the substrate more efficiently. On the other hand, the more forceful impact of the *wide* nozzle sprays occurs at the expense of somewhat higher spray temperature, which may partially counteract the enhancement of q achieved with *wide* nozzles.

In view of these results, we may infer that the surface heat extraction could be enhanced by increasing the current nozzle diameter and/or shortening its length. One should be aware, however, that changes in nozzle design affects other spray properties, such as temperature and area covered, which could pose

some practical limitations. Aiming to optimize CSC, we have recently investigated two alternative solutions: fine adjustment of the distance between the nozzle and skin [7], and sequential cryogen spraying for precise control of the cryogen mass flux [22], [23].

V. CONCLUSION

- 1) Two distinctive cryogenic spray patterns have been identified for the nozzles under study: coarser (jet-like) sprays, produced by nozzles with inner diameters (D_N) of 1.4 mm (*wide* nozzles); and finely atomized sprays (larger cone), produced by nozzles with $D_N = 0.5$ – 0.8 mm (*narrow* nozzles). Nozzle length (L_N) has but a small impact on spray shape.
- 2) A distinctive average droplet diameter D , velocity $V_{1,2}$, and temperature T with distance from the nozzle z is observed in each of these two patterns. The *wide* nozzle sprays show D ranging from 10 to 15 μ m, $V_{1,2}$ dropping from 60 to 80 m/s to <5 m/s, and T varying from -26 °C to -60 °C for the range of distances covered ($0 < z < 225$ mm). The *narrow* nozzle sprays exhibit D between 2 and 6 μ m, $V_{1,2}$ reducing from 15 to 30 m/s to <5 m/s, and T between -29 °C and -57 °C, for the range of distances covered ($0 < z < 250$ mm).
- 3) A single-droplet evaporation model represents $T(z)$ reasonably well for all nozzles. However, the model does not adequately represent $D(z)$ in the presence of recirculation zones and droplet coalescence, as substantiated by preliminary PDPA velocity measurements.

ACKNOWLEDGMENT

Insightful discussions with K. Pope, and Dr. J. Hsia, Dr. W. Verkruysse, Dr. L. O. Svaasand, and Dr. B. S. Tanenbaum are greatly appreciated. Laboratory assistance provided by Y.-H. J. Hsu and the equipment donation from Candela Corporation are also acknowledged.

REFERENCES

- [1] J. S. Nelson, T. E. Milner, B. Anvari, B. S. Tanenbaum, S. Kimel, L. O. Svaasand, and S. L. Jacques, "Dynamic epidermal cooling during pulsed laser treatment of port wine stain. A new methodology with preliminary clinical evaluation," *Arch. Dermatol.*, vol. 131, pp. 695–700, 1995.
- [2] J. H. Torres, J. S. Nelson, B. S. Tanenbaum, and T. E. Milner *et al.*, "Estimation of internal skin temperatures in response to cryogen spray cooling: Implications for laser therapy of port wine stains," *IEEE J. Select. Topics Quantum Electron.*, vol. 5, pp. 1058–1066, July/Aug. 1999.
- [3] J. S. Nelson, B. Majaron, and K. M. Kelly, "Active skin cooling in conjunction with laser dermatologic surgery: Methodology and clinical results," *Sem. Cutaneous Med. Surg.*, vol. 19, pp. 253–266, 2000.
- [4] C. J. Chang and J. S. Nelson, "Cryogen spray cooling and higher fluence pulsed dye laser treatment improve port-wine stain clearance while minimizing epidermal damage," *Dermatol. Surg.*, vol. 25, pp. 767–772, 1999.
- [5] B. Anvari, B. S. Tanenbaum, T. E. Milner, and S. Kimel *et al.*, "A theoretical study of the thermal response of skin to cryogen spray cooling and pulsed laser irradiation—Implications for treatment of port wine stain birthmarks," *Phys. Med. Biol.*, vol. 40, pp. 1451–1465, 1995.
- [6] W. Verkruysse, B. Majaron, B. S. Tanenbaum, and J. S. Nelson, "Optimal cryogen spray cooling parameters for pulsed laser treatment of port wine stains," *Lasers Surg. Med.*, vol. 27, pp. 165–170, 2000.
- [7] G. Aguilar, B. Majaron, K. Pope, L. O. Svaasand, E. J. Lavernia, and J. S. Nelson, "Influence of nozzle-to-skin distance in cryogen spray cooling for dermatologic laser surgery," *Lasers Med. Surg.*, vol. 28, pp. 113–120, 2001.

- [8] B. M. Pikkula, J. H. Torres, J. W. Tunnell, and B. Anvari, "Cryogen spray cooling: effects of droplet size and spray density on heat removal," *Lasers Med. Surg.*, vol. 28, pp. 103–112, 2001.
- [9] E. Karapetian, G. Aguilar, E. J. Lavernia, and J. S. Nelson, "Influence of cryogen spray cooling parameters on the heat extraction rate from a sprayed surface," in *Proc. SPIE*, vol. 3907, San Jose, CA, 2002, pp. 37–58.
- [10] E. Karapetian, G. Aguilar, S. Kimel, E. J. Lavernia, and J. S. Nelson, "Effect of cryogen spray droplet velocity and mass flow rate on surface cooling," *Phys. Med. Biol.*, vol. 48, pp. N1–N6, 2003.
- [11] G. Aguilar, B. Majaron, W. Verkruysse, Y. Zhou, J. S. Nelson, and E. J. Lavernia, "Theoretical and experimental analysis of droplet diameter, temperature, and evaporation rate evolution in cryogenic sprays," *Int. J. Heat Mass Transfer*, vol. 44, pp. 3201–3211, 2001.
- [12] W. Verkruysse, B. Majaron, G. Aguilar, J. S. Nelson, and L. O. Svaasand, "Dynamics of cryogen deposition in relationship to heat extraction rate during cryogen spray cooling," in *Proc. SPIE*, vol. 3907, San Jose, CA, 2000, pp. 37–48.
- [13] G. Aguilar, W. Verkruysse, B. Majaron, L. O. Svaasand, E. J. Lavernia, and J. S. Nelson, "Measurement of heat flux and heat transfer coefficient during continuous cryogen spray cooling for laser dermatologic surgery," *IEEE J. Select. Topics Quantum Electron.*, vol. 7, pp. 1013–1021, Nov./Dec. 2001.
- [14] L. O. Svaasand, L. L. Randeberg, G. Aguilar, B. Majaron, S. Kimel, E. J. Lavernia, and J. S. Nelson, "Cooling efficiency of cryogen spray during laser therapy of skin," *Lasers Surg. Med.*, to be published.
- [15] D. J. Holve, T. L. Harvill, and J. H. Hoog, "In-process particle size distribution measurements and control," in *Proc. Int. Congr. Particle Technology*, Mar. 21–23, 1995, [Online]. Available: <http://www.process-matrix.com/epcs.html>.
- [16] A. H. Lefebvre, *Atomization and Sprays*, 1st ed. New York: Taylor & Francis, 1989.
- [17] B. Anvari, B. J. Ver Steeg, T. E. Milner, B. S. Tanenbaum, T. J. Klein, E. Gerstner, S. Kimel, and J. S. Nelson, "Cryogen spray cooling of human skin: Effects of ambient humidity level, spraying distance, and cryogen boiling point," in *Proc. SPIE*, vol. 3192, San Jose, CA, 1997, pp. 106–110.
- [18] M. Orme, "Experiments on droplet collisions, bounce, coalescence and disruption," *Progr. Energy Combust. Sci.*, vol. 23, pp. 65–79, 1997.
- [19] R. Nishitani, A. Kasuya, and Y. Nishina, "In situ STM observation of coalescence of metal particles in liquid," *Zeitschrift Phys. D: Atoms, Molecules and Clusters*, vol. 26, pp. S42–S44, 1993.
- [20] W. D. Bachalo, "Method for measuring the size and velocity of spheres by dual-beam light-scatter interferometry," *Appl. Opt.*, vol. 19, pp. 363–370, 1980.
- [21] B. Majaron, S. Kimel, W. Verkruysse, G. Aguilar, K. Pope, L. O. Svaasand, E. J. Lavernia, and J. S. Nelson, "Cryogen spray cooling in laser dermatology: Effects of ambient humidity and frost formation," *Lasers Surg. Med.*, vol. 28, pp. 469–476, 2001.
- [22] B. Majaron, G. Aguilar, B. Basinger, L. L. Randeberg, L. O. Svaasand, E. J. Lavernia, and J. S. Nelson, "Sequential cryogen spraying for heat flux control at the skin surface," in *Proc. SPIE*, vol. 4244, San Jose, CA, 2001, pp. 74–81.
- [23] B. Majaron, L. O. Svaasand, G. Aguilar, and J. S. Nelson, "Intermittent cryogen spray cooling for optimal heat extraction during dermatologic laser treatment," *Phys. Med. Biol.*, vol. 47, pp. 3275–3288, 2002.



Guillermo Aguilar received the B.S. degree in mechanical engineering from the National Autonomous University of Mexico (UNAM), Mexico City, Mexico, in 1993, and the M.S. and Ph.D. degrees in mechanical engineering from the University of California, Santa Barbara, in 1995 and 1999, respectively.

In 1999, he was a Post-Doctoral Researcher at the Beckman Laser Institute and the Department of Chemical and Biochemical Engineering and Material Science, both at the University of California, Irvine (UCI). He is currently an Assistant Professor at the Department of Biomedical Engineering, UCI. His research interests include cryogen spray atomization and heat transfer, application of cryogen sprays and laser irradiation in dermatology, and therapeutic applications of lasers in dermatology and reconstructive surgery.



photothermal radiometry.

Boris Majaron received the B.S., M.S., and Ph.D. degrees in physics from the University of Ljubljana, Ljubljana, Slovenia, in 1985, 1989, and 1993, respectively.

Since 1993, he has been with the Joef Stefan Institute, Ljubljana, Slovenia. His research experience includes laser spectroscopy of strongly doped laser materials, nonlinear optics, and laser technology. His research in the field of biomedical optics involves therapeutic laser applications for dermatology and dentistry, cryogen spray cooling, and pulsed



Emil Karapetian received the B.S. and M.S. degrees in chemical and materials science from the University of California, Irvine, in 2000 and 2002, respectively.

He is currently with Applied Medical Company, Rancho Santa Margarita, CA.



Enrique J. Lavernia received the B.S. degree in solid mechanics from Brown University, Providence, RI, in 1982, and the M.S. degree in metallurgy and the Ph.D. degree in materials engineering from the Massachusetts Institute of Technology, Cambridge, in 1984 and 1986, respectively.

He is currently Dean of the School of Engineering and Full Professor in the Department of Chemical Engineering and Material Science, University of California, Davis. His research interests are the processing of structural materials and metal matrix

composites with particular emphasis on solidification fundamentals, rapid solidification processing, spray atomization and deposition of structural materials, solidification processing of metal matrix composites, and mathematical modeling of advanced materials and processes.



J. Stuart Nelson received the M.D. degree from the University of Southern California, Los Angeles, and the Ph.D. degree from the University of California, Irvine.

He is Associate Director at the Beckman Laser Institute and Medical Clinic and a full-time Professor in the Departments of Surgery, Dermatology, and Biomedical Engineering at the University of California, Irvine. His research interests include studies at both the basic science and applied levels.

The basic science studies fall into two specific areas: 1) the biophysics of laser interaction with biological tissues and 2) the understanding of structural changes produced in tissues by laser light. At the applied level, his research objectives are in developing new approaches to the diagnosis and treatment of diseases amenable to laser therapy.